Origins of Life and Evolution of Biospheres (2005) 35: 429–445 © Springer 2005

ICE AND THE ORIGIN OF LIFE

HAUKE TRINKS[1], WOLFGANG SCHRÖDER[1] and CHRISTOF K. BIEBRICHER[2,*]
[1]*Technical University Hamburg-Harburg, D-21071 Hamburg, Germany*
[2]*Max-Planck-Institute for Biophysical Chemistry, Am Fassberg, D-37077 Göttingen, Germany*
*(*author for correspondence, e-mail: cbiebri@gwdg.de)*

(Received 20 July 2004; accepted in revised form 3 January 2005)

Abstract. Sea ice occurs abundantly at the polar caps of the Earth and, probably, of many other planets. Its static and dynamic properties that may be important for prebiotic and early biotic reactions are described. It concentrates substrates and has many features that are important for catalytical actions. We propose that it provided optimal conditions for the early replication of nucleic acids and the RNA world. We repeated a famous prebiotic experiment, the poly-uridylic acid-instructed synthesis of polyadenylic acid from adenylic acid imidazolides in artificial sea ice, simulating the dynamic variability of real sea ice by cyclic temperature variation. Poly(A) was obtained in high yield and reached nucleotide chain lengths up to 400 containing predominantly $3' \rightarrow 5'$ linkages.

Keywords: replication, RNA world, poly(A), prebiotic chemistry, ribozymes

1. Introduction

The origin of life on Earth has been a drama with many acts, where the different acts may have taken place under very different conditions (Arrhenius *et al*., 1999). For the synthesis of monomers, a temperature range from around 250 °C in hot underwater springs (Macleod *et al*., 1994) to −250 °C in frozen matter in space (Munoz-Caro et al., 2002) has been proposed and supported by experiments.

However, in other proposed steps of the origin of life the temperature range permitted by the chemical laws is rather limited (Moulton *et al.*, 2000). This applies for one of the most conspicuous criteria for life, proliferation, i.e., a mother organism produces offspring that has nearly identical properties. The underlying molecular phenomenon is replication of the genome. There is general agreement that RNA is the older form of the nucleic acids, since, in contrast to deoxyribose, ribose is readily formed by aldol condensation, and the nucleophilicities of the 2′,3′-OH residues of nucleotides is much higher than those of the corresponding deoxyribonucleotides (Lohrmann and Orgel, 1976). Furthermore, DNA replication still needs the synthesis of RNA, particularly in chain initiation, where phosphodiester formation takes place between the first two nucleotides of the chain.

It was one of the greatest triumphs in prebiotic chemistry that Orgel and collaborators succeeded to perform non-enzymic RNA replication in vitro. The ability to duplicate are inherent properties of nucleic acids, in particular of the nucleobases. It

is based on formation of a regular, quasi-crystalline structure where base-stacking and base-pairing are the main forces.

In a series of experiments, Orgel and collaborators investigated non-enzymic replication of RNA in vitro (reviewed in Orgel, 1987; Schwartz *et al.*, 1987; Joyce, 1987). It was crucial for the reactions to succeed to find activated nucleotides that reacted at a rate suitable for laboratory studies, because nucleoside triphosphates were too inert to condense at measurable rates. Nucleotide imidazolides were found to be suitable (Lohrmann and Orgel, 1977) even though it is unlikely that they are formed under prebiotic conditions. The conditions for the non-enzymic conditions were temperatures around the freezing point and rather high ionic strength (Inoue and Orgel, 1982). The low temperature is required because the next base for chain elongation must stack upon the double helix and remain there for sufficient time for phosphodiester bond formation. The high ionic strength is necessary to reduce the repulsion of template and substrates which both carry negative charges.

These experiments have recently been reinvestigated by several scientists incubating the reactions at constant temperatures below the freezing point. Stribling and Miller (1991) cooled down artificial sea water mixed with monomers to the constant temperature of $-18\,^{\circ}$C. After time intervals ranging from 48 hours to 56 days, the reaction products were analysed. Under these conditions, template-directed RNA synthesis products were similar to what had been obtained previously reported for temperatures of $4\,^{\circ}$C, i.e. complementary RNA oligomers with chain lengths of up to 12–15 were obtained. Monnard *et al.* (2003) performed template-free poly(A) synthesis experiments at a constant temperature of $-18\,^{\circ}$C for time periods of up to 38 days. In these experiments, at low ionic strength and with the reaction mixture doped with Pb^{2+} and Mg^{2+} ions, oligo(A) with chain lengths of up to 17 were obtained. Higher ionic strength inhibited the reaction (Monnard, personal communication and Monnard *et al.*, 2002) to such an extent that only dimers were obtained, leading to the suggestion that RNA replication may have originated in ponds of fresh water on the early continents and not in the sea. Vlassov *et al.* (2004) pointed out that RNA degradation is markedly slowed down at low temperatures, preserving RNA molecules of significant complexity. Corresponding experiments with ribozymes were performed for time periods of some hours at temperature ranges of $-4\,^{\circ}$C to $-12\,^{\circ}$C in solutions containing 10–100 mM NaCl. These results suggest that complex RNAs could have evolved at temperatures below the freezing point.

In this article, we propose that frozen sea water with realistic temperature variations is a particularly suitable matrix for steps leading to life, notably the synthesis of high molecular weight RNA. A description of the chemical and physical conditions in sea ice is given in respect to their usefulness for pre-biotic synthesis. Temperature fluctuation between -7° and -24° were induced. Under these conditions, the synthesis of poly(A) on a poly(U) template led to nucleotide chain lengths of up to 400, a size sufficient for functional RNA.

2. Results

2.1. Sea ice, an environment with special properties

One of the authors (H.T.) has undertaken two expeditions, 1999–2000 and 2002–2003, to the north of Spitsbergen, to investigate the properties of the sea ice in the run of the temperature and light cycles between winter and summer with periods of 4 months dark and light (Trinks, 2001a). Air temperature, air pressure and light strength were recorded continuously. The microstructure of the ice material was investigated at different temperatures, ice thicknesses and ice depths by light and fluorescence microscopy at magnifications up to 1000. Temperatures, pressures, pH-values, salt concentrations, electrical potentials, light strength and light polarization effects at different depths of the ice lumps were measured. Various organic compounds were injected into the ice layer and their behaviour was observed. Psychrophilic organisms were collected from the ice and characterized in the laboratory. A huge number of microorganisms were found in the ice, most of which were still previously unknown (Groudieva *et al.*, 2004). The found characteristics of the sea ice, (summarized schematically in Figure 1) led to the hypothesis that the conditions in sea ice may offer interesting features that are advantageous for some steps in the origin of life (Trinks, 2001b).

The formation of sea ice is a complex process described in numerous publications (reviewed in Wettlaufer *et al.*, 1999). When sea water is cooled down by cold air to temperature below $-1.8\,^{\circ}$C, freezing begins. The start of freezing depends on the heat capacity of the water layer and water convection. In contrast to fresh water, sea water has its maximal density near the freezing point so that the entire layer must cool down to the freezing point. Many small crystals of salt-free water with lengths of a few mm grow in the cool water layer. They float towards the surface because their specific density is below the density of the surrounding salt water. At further cooling, the resulting thick ice slurry forms lumps with rounded surfaces.

Within 8 months after the warmest month, July, the sea ice layer grows to a thickness of 1 to 2 m in the northern regions of Spitsbergen. During formation of the ice, the salt concentration of the liquid brine located between the tiny solid ice crystals rises from about 3.5% up to 25% salt. The concentration of the brine is displayed in Table I (Sakshaug *et al.*, 1994). At a certain temperature, water is removed by freezing until the equilibrium brine concentration is reached. The brine is concentrated within the ice structure in small channels and caviols with diameters from 10 to 100 μm. In the warmer period of summer the ice may melt partially. During this process the caviols and channels become wider.

If the temperature goes to rather low temperatures, the solubility limit of some salts is reached and crystals of salts precipitate (Assur, 1958), e.g., $CaCO_3$ at $-3\,^{\circ}$C, Na_2SO_4 at $-10\,^{\circ}$C or NaCl at $-23\,^{\circ}$C. When the temperature rises again, the salt crystals are not redissolved immediately. Particularly $CaCO_3$ remains as small solid

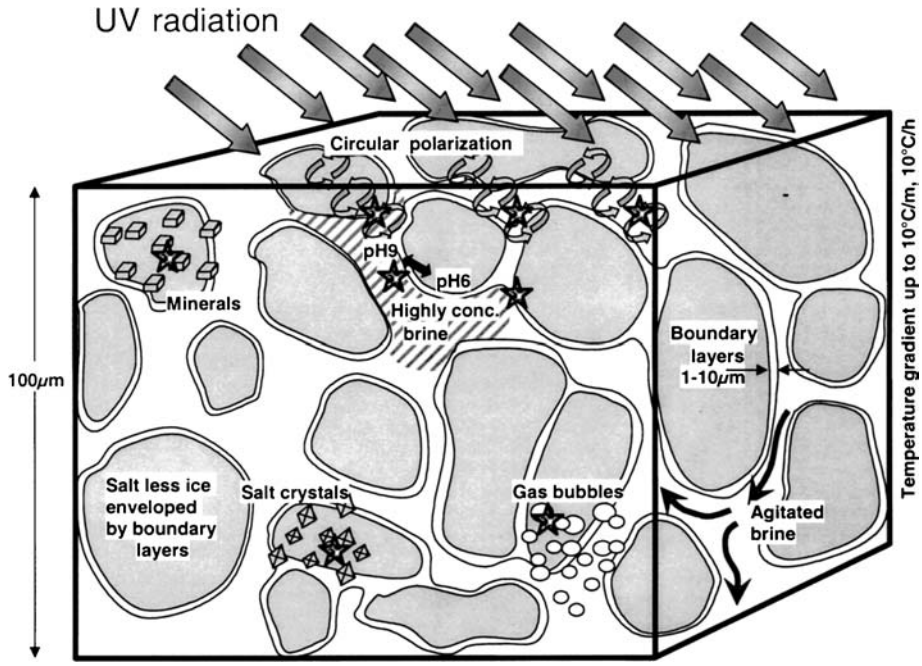

Figure 1. Model of a sea ice reactor (volume 100 μm $\times$ 100 μm $\times$ 100 μm). The model depicts microstructure and properties of sea ice. The three phase system consists of salt-less ice crystals enveloped by membrane-like layers, highly concentrated brine, gas bubbles (presumably CO_2) and salt crystals. Temperature gradients up to 10 °C/h and 10 °C/m cause mechanical agitation of the brine, strong gradients in pH and electrical potentials, energy transport and exchange, freezing and melting, crystallizing and dissolving. UV light from the sky, partly circular polarized by the influence of the ice structure, is an energy source particularly active at the surface of the reactor. Regions with possible catalytic action are marked with asterisks.

particles for some hours in the melted ice water. Gases, in particular carbon dioxide (Semiletov *et al.*, 2004) dissolve in the brine and gass out as very tiny bubbles (diameter 1 to 10 μm) when the -30 °C cold ice system warms up. The boundary between solid crystals and the brine seems to have a special interface structure which is clearly visible in the light microscope by its refractive properties. When the temperature rises and part of the ice melts, such structures often remain visible for up to 30 minutes after the ice has disappeared. Under the light microscope, these structures resemble membranes that form vesicles or envelop cells (Engemann *et al.*, 2004).

The described microstructure characterized by narrow channels and caviols filled with liquid brine was observed not only in sea ice, but also in the ice of brackish water with only 0.5% salt concentration and even in glacier ice with very low salt content. By physical reasons, the freezing process of water with salt concentrations between less than 0.1% and up to 3.5% leads to quite similar results.

TABLE I
Concentration of ions in natural sea water (Sakshaug *et al.*, 1994)

Ions in sea salt	Conc. (g/l)	Conc. (mMol/l)	Chem. symbol
Chloride	19.87	560	Cl^-
Sodium	11.05	480	Na^+
Magnesium	1.32	54.3	Mg^{2+}
Sulfate	2.784	28.9	$SO_4{}^{2-}$
Calcium	0.422	10.5	Ca^{2+}
Potassium	0.416	10.6	K^+
Bromide	0.068	0.851	Br^-
Bicarbonate	151.0	2.33	$HCO_3{}^-$
Strontium	0.0085	0.097	Sr^{2+}
Borate	4.5	0.417	$H_3BO_3{\cdot}B(OH)_4{}^-$
Fluoride	0.0014	0.074	F^-

The brine is threefold concentrated at $-10\,^\circ$C, fivefold at $-20\,^\circ$C. The upper limits of the Ca^{2+}- and $HCO_3{}^-$ concentrations are 13.1 mM and 6.55 mM, repectively, due to the solubility limit of $CaCO_3$. $MgCl_2$ and Na_2SO_4 reach their solubility limits close to $-20\,^\circ$C.

2.2. Physical and chemical properties of sea ice

As judged from numerous microscopic observations made in different ice layers, 1 m^3 sea ice contains approximately 10^{14} to 10^{15} compartments or a network of channels with a combined surface of 10^5 to 10^6 m^2. When the air temperature rapidly changes or ice layers break up, local temperature gradients in the ice material were formed with values up to $10\,^\circ$C/h and $10\,^\circ$C/m. The resulting density changes in the ice led to local pressure gradients and corresponding motion of the liquid brine in the tiny channels. By microscopical observations the currents of brine were estimated to reach values of 5×10^{-4} m/s. The macroscopic pressure variation between different ice layers was measured with a pressure transducer and found to reach values of up to 5×10^6 N/m^2.

Sea water has a pH value of about 8.2. In sea ice, however, pH gradients between pH 5 and pH 9 were measured and reported (Bronshteyn and Chernov, 1991). pH values were made visible using the pH indicators mixed into sea water before freezing. The pH of the brine dripping out of pieces of sea ice at $-15\,^\circ$C reached a value of 9 while the pH of the drained ice structures ranged from pH 5 to pH 6. Due to strong salt gradients between salt-less ice crystals and highly concentrated brine (Figure 2 top), electrical potential differences of up to 50 mV have been measured (Figure 2 bottom), in agreement with reported values (Steponkus *et al.*, 1984).

Sea ice interacts with organic compounds. A dye mixture injected into a small hole at the surface of an ice layer diffused into the channels and was separated by chromatographic forces into their components. This illustrates the fractionating

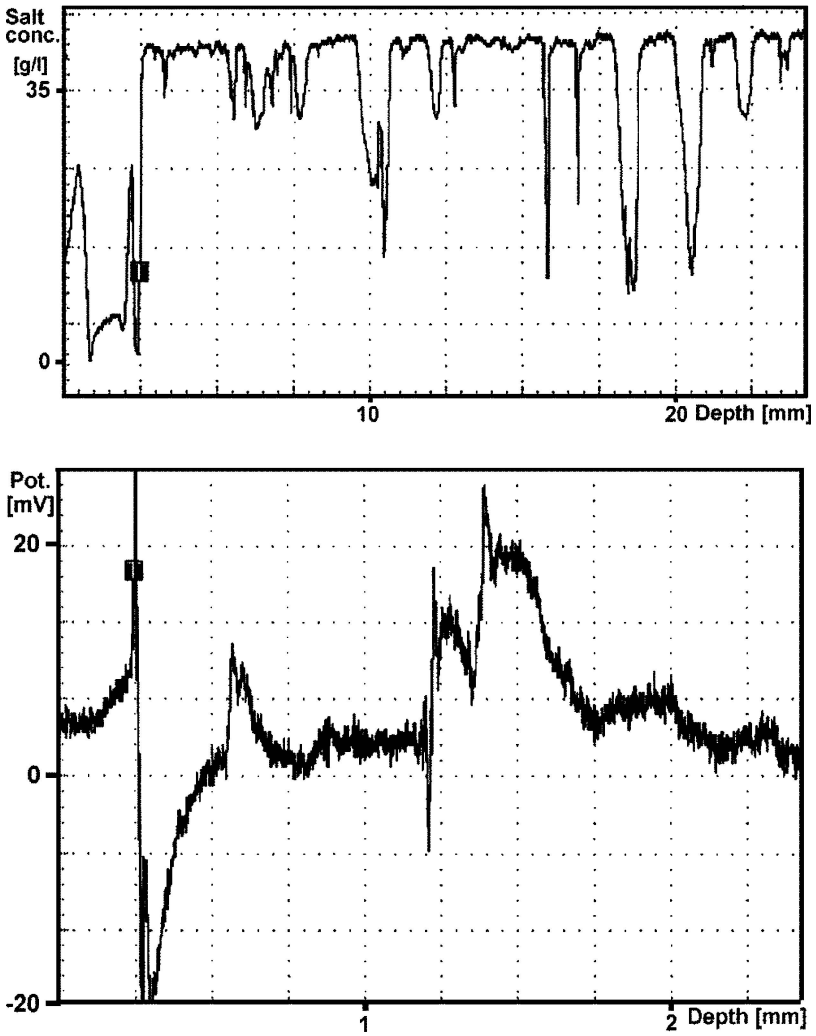

Figure 2. Properties of sea ice. Top: Salt concentration in sea ice ($-5\,^{\circ}$C). An electrical conductivity-measuring probe was moved through ice with a speed of 10 cm/s. The measured values were found to vary in a wide range, corresponding to salt concentrations from almost zero to 40 g/l. Bottom: Electrical potentials in sea ice ($-5\,^{\circ}$C). An electric probe (diameter 100 μm) was moved through ice with a speed of 10 cm/s and voltage impulses from +20 mV to −20 mV were recorded.

power of the ice structure. In a similar way, a mixture of various amino acids were injected into the ice reactor. After 6 hours samples of ice were taken at different locations in the ice and analysed. Amino acids were partly separated one from another by chromatography in ice.

RNA labeled by ethidium bromide and dissolved in sea water was observed to concentrate after freezing in the channels (Figure 3) and to adhere particularly

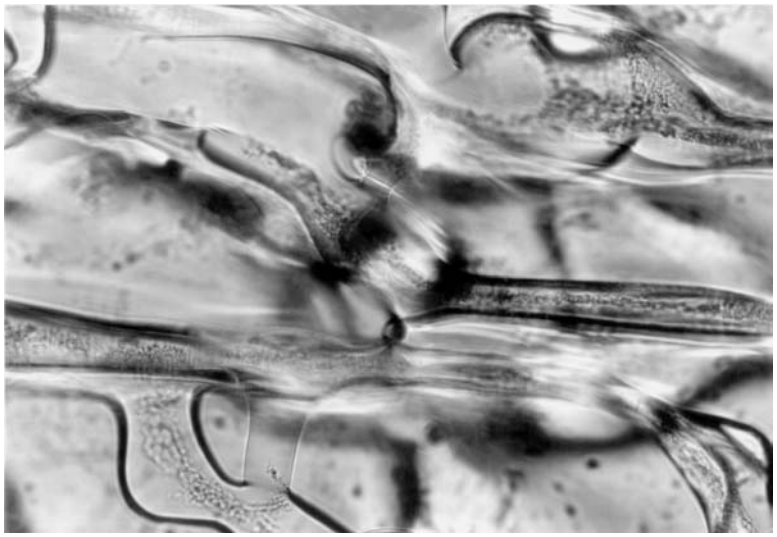

Figure 3. Concentration of RNA in sea ice. A complex of yeast RNA and ethidium bromide was dissolved in sea water. During freezing, the RNA was concentrated in the channels (area 25 μm $\times$ 50 μm, $-10\,^{\circ}$C) and formed aggregates visible in the fluorescence microscope.

at the liquid-solid boundaries. When the ice has been re-melted after some hours, insoluble RNA aggregates formed a net of strings still showing the structures of the brine channels. At low temperatures of about $-30\,^{\circ}$C, the RNA seemed to prefer precipitating on the surfaces of salt crystals growing in the highly concentrated brine. When the temperature of the ice rose, the salt crystals redissolved in the liquid, while the RNA aggregates remained insoluble indicating the size and the position of the vanished salt crystals.

The properties of sea ice and its possible role in the origin of life has been reviewed previously in more detail by the authors (Trinks *et al.*, 2003). The experimental results obtained during the expeditions as well as the review of the vast literature in this field suggest in the opinion of the authors that this particular environment may have served as a potential reactor with excellent conditions for primordial steps to life.

2.3. Non-enzymic RNA replication

2.3.1. *Reaction*

Prebiotic experiments can of course not be performed in a natural habitat: living organisms would rapidly metabolize the reagents. We worked thus in the laboratory with commercially available sea water salt that is made from chemically pure chemicals and is devoid of organic material. The low temperatures were supplied by a normal freezer. Cyclic temperature changes between –7 and $-24\,^{\circ}$C were

effected by switching the freezer on and off in a cycle time of 4 h. At the temperature maximum, the ice is still not totally melted, while at the temperature minimum an eutectic solid with very little residual liquid is obtained.

As a reaction, we performed a poly(U)-directed polymerisation of 5′-adenylic (2-methyl)imidazolides as described by Orgel and collaborators (Lohrmann and Orgel, 1977; Inoue and Orgel, 1982), but in sea ice, sample 1 unbuffered, sample 2 buffered with 0.1 M (1)-methylimidazol buffer, pH 8.0. Chemical reactions are known to proceed at reduced rates at lower temperature; so for the preliminary experiment an ample time span was chosen for the reaction to proceed.

After approximately 1 year, the frozen samples were thawed and analysed. To exclude microbial contamination, the solution was checked by light microscopy, no precipitates, visible aggregates or microorganisms were found.

Thin layer chromatography on PEI-cellulose plates (not shown) revealed, among substantial amounts of unreacted monomer, oligomers of all lengths and, as main product, polymer. The products were freed from salt and unreacted monomer by gel chromatography on a NAPS column. This separation removes also oligonucleotides of small chain lengths. From the absorbance at 260 nm, the mass of the nucleic acids has doubled in sample 1, while the increase in mass was much less in sample 2. In part of the sample, the poly(U) template was destroyed by the RNase A treatment followed by phenol extraction and alcohol precipitation. Since the specificity of RNase for pyrimidines is high but limited, the optimal amount of RNase was determined experimentally.

2.3.2. *Composition of the Products*

The degradation products of poly(U) were removed by gel filtration on a NAPS column.

Extensive alkaline degradation of the products revealed by thin layer chromatography (Figure 4) mainly Ap and, in smaller amounts, pAp and Ado. UMP was only detected as a trace, approximately 1% of the total mass in sample 1 and 5% in sample 2.

The synthesis of poly(A) in the ice reactor and the results of the electrophoretic separation were confirmed by analysis with capillary zone electrophoresis mass spectrometry (CZE/MS) and matrix-assisted laser desorption ionization time of flight mass spectrometry (MALDI/TOFMS).

To test whether the high molecular weight material is composed of A residues, the product was partially degraded by limited alkaline hydrolysis and analysed by CZE/MS. Again, oligomers with chain lengths between 2 and 8 were found; no nucleotides other than A, in particular U from residual template, were detected (Figure 5).

In the MALDI/TOFMS spectra recorded in the lower mass range measuring mode ($<$3500 Da) only fragment ions that were derived from poly(A) were detected (Figure 6 top). Signals from material containing U were absent. Signals rapidly decreased in intensity from dimers to decamers, due to the decreasing response of

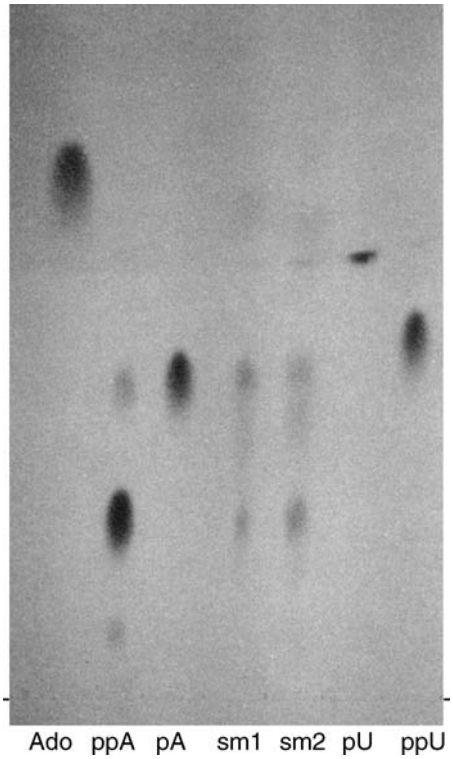

Figure 4. Thin layer chromatogram of alkali-degraded poly(A) products. 20 μg desalted reaction sample 1 were incubated with 2 ng RNase A at 37 °C for 10 min, phenol extracted, precipitated with EtOH, redissolved in water and purified over a NAPS column. Alkali degradation was with 20% piperidin for 5 h at 50 °C. TLC was on PEI cellulose sheets developed with 0.55 M $(NH_4)_2SO_4$.

the mass spectrometry at higher chain lengths. Measurements in the high mass range mode indicated material up to the upper mass limit of 1.4×10^5 Da, corresponding to poly(A) of the chain length 420 (Figure 6 bottom). However, MALDI/TOFMS only gives qualitative results, due to its mass-dependent response.

2.3.3. *Chain Length of the Products*

Polyacrylamide gel electrophoresis followed by staining the RNA with toluidine blue revealed for the native nucleic acids a relatively narrow band at a very high molecular weight (Figure 7). After treatment with RNase A a broad distribution of poly(A) strands with chain lengths up to more than one hundred was obtained. After further incubation with RNase A, the nucleotide chain length of the poly(A) was reduced. Therefore, the nucleotide chain lengths of the synthesized products are higher than determined. The chain lengths are suprisingly high, much higher than previously observed in the polymerisation of activated AMP on poly(U) or the polymerisation of activated GMP directed by poly(C) (Lohrmann and Orgel,

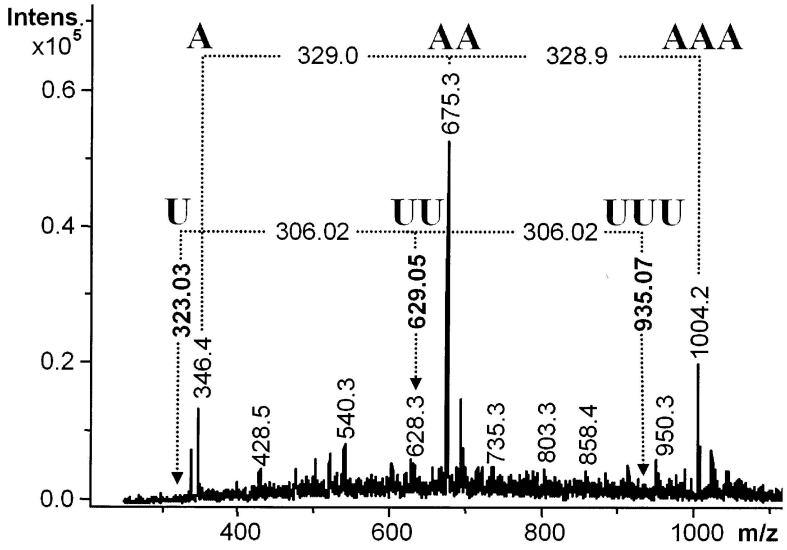

Figure 5. CZE/MS analysis in negative ion mode. Partially degraded product was separated by capillary zone electrophoresis and the products analysed by mass spectroscopy. Shown is the trimer, which only gives signals for $(Ap)_3$ and its fragmentation to Ap and $(Ap)_2$. No signals are seen at the positions expected for $(Up)_3$ and its degradations products (indicated by arrows).

1977; Inoue and Orgel, 1982). While the length distribution of the products was essentially the same in buffered and unbuffered solutions, the unbuffered samples had a much higher yield. Since the pH value was about the same in both samples, it may indicate that the pH gradients formed in the ice (as mentioned above) have a positive effect on the reaction rate. It is not excluded, however, that the buffer substance used acts as an inhibitor. Little is seen at the bottom of the gel, but this may be an artefact of the staining procedure: Shorter oligonucleotides (<20) are neither efficiently fixed in the gel nor do they stain normally.

The indicated chain length of the products is too high to achieve a satisfactory resolution by ion exchange HPLC. Therefore, the poly(A) products, shown to contain no other nucleotides, were labeled by phosphorylating the 5′ termini with [^{32}P]-phosphate, with and without prior dephosphorylation. Newly synthesized material has 5′-terminal phosphates, while the 3′-terminal fragments produced by overdigestion with RNase A contain already 5′-terminal OH and can be phosphorylated without prior dephosphorylation. Therefore, the difference in phosphorylation with or without prior dephosphorylation should also give some information of the poly(A) degradation. The electrophoretic separation of the labeled products showed oligonucleotides of chain lengths of up to 150 A residues (Figure 8 top: autoradiogram, bottom: densitogram of the autoradiogram in the chain length range of 40–160 nucleotides). The intensity of the bands decreases with increasing chain lengths. Nevertheless, the results shown in Figures 7 and 8 confirm each other: to

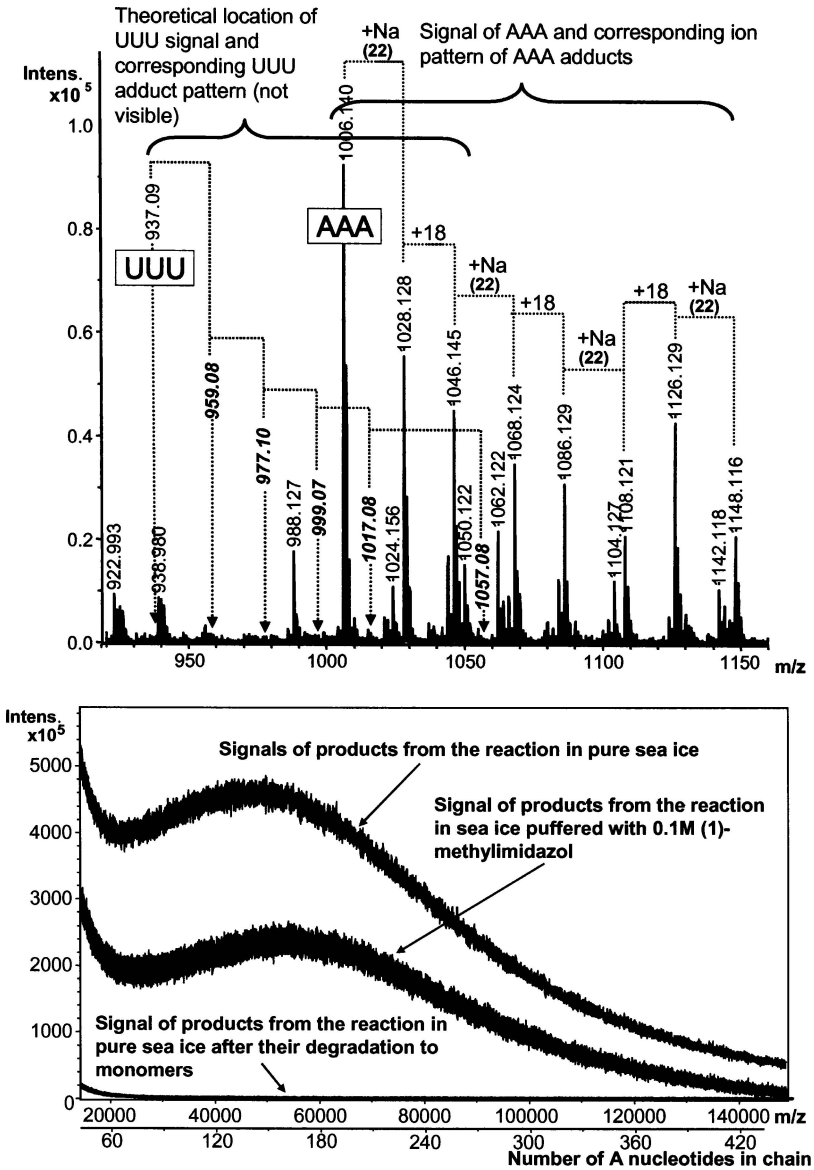

Figure 6. MALDI/TOF/MS analysis of product in positive ion mode. Top: Fragmentation of the product poly(A) takes place and allows identification of the polymer composition. In this figure $(Ap)_3$ and its complexes is seen. Fragmentation products containing U were not detectable (arrows). Bottom: Measurements in the high mass range mode show ions with molecular weights up to 1.4×10^5 Da, corresponding to chain lengths up to 420. The upper line is the product of poly(A) synthesis in unbuffered sea ice, the lower line the synthesis product in buffered sea ice, the zero line is product extensively degraded by alkali. The monomer line reveals in the MALDI spectrum a chemical noice of $<1\%$, in contrast to the undegraded polymer signals, indicating that the amplitude of the MALDI spectra is generated by high molecular weight polynucleotides.

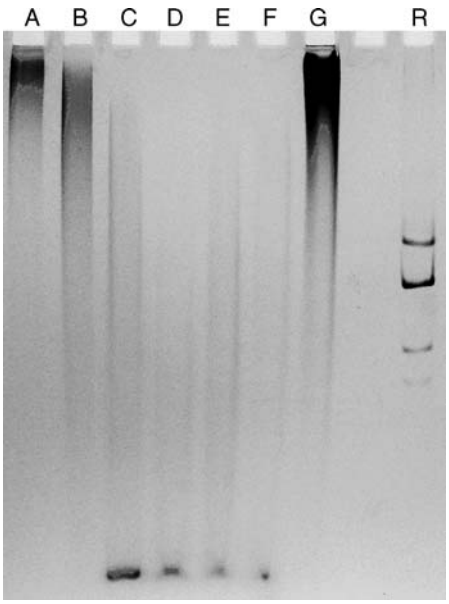

Figure 7. Gel electrophoresis of the non-enzymic nucleic acid synthesis. Gel electrophoresis on a 8% polyacrylamide gel. Lanes A and B are sample 1 and sample 2 from the reaction without further purification; For C and D, 20 μg desalted reaction sample 1 and 10 μg sample 2 were treated with 2 ng each of RNase A and incubated at 37 °C for 10 min. E and F as C and D, but incubation for 40 min; lane G: 40 μg poly(U); lane R: 4 μg MDV-1 (nucleotide chain length 220) double and single strand.

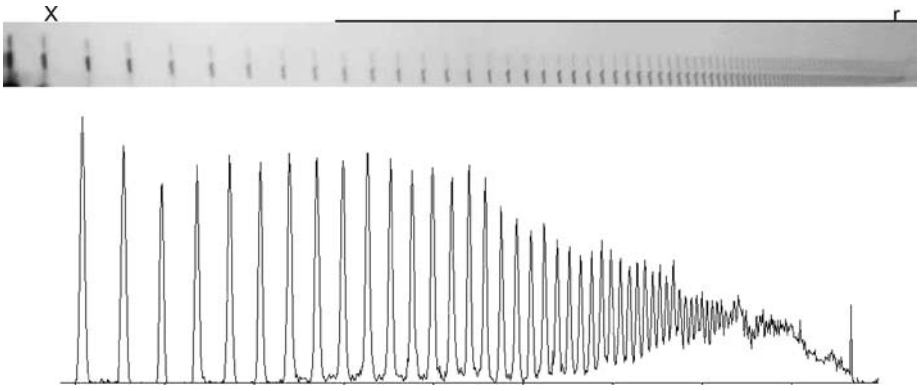

Figure 8. Top: Autoradiogram of the gelectrophoretic separation of 5′-labeled oligonucleotides. The poly(A) material described in Figure 4 was dephosphorylated, re-phosphorylated with [γ-^{32}P]-ATP and subjected to gel electrophoresis as described in the Methods part. Upper lane: without dephosphorylation, lower lane: with prior dephosphorylation. X and r are the positions of the dye xylene cyanol blue FF (runs approximately with the 29mer) and 5S rRNA (chain length 119) from yeast, respectively. Bottom: Densitogram of the part of the lower line in the autoradiogram marked by the line.

obtain the mass of the oligonucleotides, one has to multiply the ends by the chain length number. About 1/3 of the intensity was observed without prior dephosphorylation. This suggests that during the exhaustive degradation of the poly(U) template by RNase A substantial degrading of the poly(A) product takes place. The chain lengths found are thus lower bounds.

Alcohol precipitation of the nucleic acids directly from the salt solution gave a heavy precipitate which did not redissolve completely in water; part of the solution needed warming to 50 °C to dissolve. Nucleic acids were found in the soluble as well as in the less soluble fraction; electrophoresis showed that the less soluble fraction contained preferentially the high molecular weight RNA.

After exhaustive digestion of the poly(A) product with RNase I from *E. coli* followed by thin layer chromatography only about 5% dimer was found in sample 1 while about 40% dimer was found in sample 2. Neither higher oligomers nor UMP were detectable. Therefore, the linkage is predominantly $3' \rightarrow 5'$ in sample 1, while substantial amounts of $2' \rightarrow 5'$ linkage was found in sample 2. If the linkages would have been distributed at random, then higher chain lengths of oligo(A) should have been found in sample 2. Apparently the linkage is not distributed at random, possibly due to sterical reasons.

3. Discussion

In this paper, we describe the properties and the behavior of real sea ice under natural conditions. Sea ice shows a complex multi-phase structure containing solid ice crystals and mineral particles, liquid brine and tiny gas bubbles. Particularly in the close neighbourhood of the manifold boundary layers, strong local gradients of pH values, ion densities and electrical potentials occur. In natural ice, temperatures fluctuate permanently, constantly shifting the phase boundaries. The brine flows in contracting and expanding tiny channels; the mineral particles and crystals grow or disappear; condensation effects and energy flows occur due to freezing or melting processes; and finally, sorting and de-mixing effects of the various reaction partners dissolved in the brine channels takes place. Under these processes sea ice grows older in the run of the year, changing its macro- and microscopic structure without return to the starting point of the first freezing. It was concluded that laboratory experiments with sea ice should be performed for long time periods with cyclic temperature fluctuations between -7 °C and -24 °C, from an fluid ice slurry to a nearly eutectic state with almost no liquid brine left. Salt concentration gradients are produced ranging from sweet water to highly concentrated brines, where the solubility limits of most salts contained in sea water were exceeded.

Using an ice reactor in the laboratory under such realistic conditions, we succeeded in the non-enzymatic synthesis of poly(A) with chain lengths and linkage fidelities that have hitherto not been achieved.

Although there is no proof, the synthesis is likely directed by the poly(U) template. Monnard *et al.* (2003) reported the condensation of adenylic imidazolide to oligo(A) without template in ice. Addition of salt reduced the condensation rate drastically. It is possible that formation of a primer is the rate-determining step and occurs preferentially without template. Once a primer of a sufficient length is produced, it binds strongly to the poly(U), and, taking the results of Monnard *et al.* (2003) into consideration, it is unlikely that further elongation takes place without participation of template.

The incubation time was rather long, about a year. Since no kinetic study has been made, the required period is not known, but after a reaction time of 3 months gel electrophoresis after RNase treatment revealed no detectable polymers, while the gel electrophoresis after 1 year suggests that the poly(U) template has been used up entirely.

This is a preliminary study which shows that a sea ice reactor is feasible for RNA replication experiments, but a thorough mechanistic analysis of the reaction in sea ice is still missing. It seems plausible that temperature fluctuations are important for the reaction (Trinks *et al.*, 2003), but this has not yet been proven. More work is in progress, but since the time spans for the observation are rather long, we wanted to present our results before all details have been determined.

Many different locations on the primitive earth habe been discussed as possible places for the origin of life. Experimental investigation on natural sea ice and the successful poly(U)-directed poly(A) synthesis lead us to propose sea ice as a matrix promoting the evolution of primitive life, be it on this planet or at another suitable location in space.

4. Materials and Methods

5′-Adenyl (2-methyl)-imidazolide was synthesized as described (Joyce *et al.*, 1984).

Reactions were performed in an ordinary household freezer that was switched on and off in a 4 h cycles. Temperatures were recorded with a Pt100 resistor. At the highest temperatures, a large part of the mixture is in liquid state while at the temperature minimum nearly eutectic conditions are achieved.

For poly(A)-synthesis in the ice reactor, the solution contained in 1 ml:

(1) 35 mg sea salt; 3.3 mg poly(U) (10 μmoles U residues); 4.3 mg 5′-adenyl (2-methyl)-imidazolide (10 μmoles);
(2) as (1), but in 0.1 M 1-methyl-imidazol-HCl buffer (pH 8.0).

After the reaction, the sample was desalted by exclusion chromatography on NAPS columns with buffer TM (0.01 Tris.HCl buffer, pH 7.4, 0.1 mM EDTA). From the absorbance at 260 nm, the masses of the nucleic acids was calculated for sample 1 to be 7.5 mg, for probe 2 3.8 mg. Thus, the nucleic acid mass in sample 1

has more than doubled, while the synthesised material in sample 2 was much less. The poly(U) template was destroyed by digestion with RNase A (2 mg/ml RNA, 1.5 μg/ml RNase) for 1 h at 37 °C. RNase was removed by extracting twice with water-saturated phenol. Degraded poly(U) was removed by purification with a NAPS column, which also removes salts and short oligo(A). All reactions were done in duplicate.

Partial alkaline degradation was done by incubating the poly(A) product in 20% piperidine for 40 min at 50 °C. For extensive degradation, the incubation time was 5 h. Thin layer chromatography was performed on washed PEI-cellulose plates containing a fluorogen at 260nm and developed with 0.55 M $(NH_4)_2SO_4$. After drying, the separation was checked under a UV illuminator.

Capillary zone electrophoresis mass spectrometry (CZE/MS, Esquire300 plus, Bruker Daltonics): The partially degraded product was separated by capillary zone electrophoresis in a 50 cm fused silica capillary with a buffer of 100 mM $(NH_4)_2CO_3$ at 15 kV and mass spectra were recorded in full negative ion scan mode between 50 and 3000 Da.

Matrix-assisted laser desorption ionization time of flight mass spectrometry (MALDI/TOFMS, Ultraflex-TOF, Bruker Daltonics): The RNA product was embedded in hydroxypicolinic acid in 5 mM ammonium acetate and ionized with a N_2 Laser at 337 nm to record mass spectra in positive ion mode in the range of 1 to 140,000 Da.

Radioactive labeling: 0.7 μg poly(A) product was dephosphorylated with 10 units alkaline phosphatase from shrimp (Roche Biochemicals) for 120 min at 37 °C. The phosphatase was destroyed by heating the solution for 15 min at 65 °C. The dephosphorylated RNA was radioactively labeled with 10 pmol ATP containing 5 μCi [γ-^{32}P]-ATP by 10 units T4-polynucleotide kinase for 30 min at 37 °C. An aliquot was loaded onto a 20% polyacrylamide gel (200 mm $\times$ 800 mm $\times$ 1 mm) containing 7 M urea in running buffer (50 mM tris, 50 mM boric acid). Electrophoresis was for 4 h at 3000 V and autoradiography for 1 d at -20 °C. The autoradiogram was scanned and analyzed by densitometry.

Linkage was tested by exhaustive digestion of the poly(A) product with RNase One (Promega) according to the conditions of the supplier, followed by thin layer chromatography as described above.

Acknowledgement

We thank Dr. Leslie Orgel for valuable suggestions.

References

Arrhenius, G., Bada, J. L., Joyce, G. F., Lazcano, A., Miller, S. and Orgel, L. E.: 1999, Origin and Ancestor: Separate Environments, *Science* **283**, 792.

Assur A.: 1958, Composition of Sea Ice and its Tensile Strength, in *Arctic Sea Ice,* U.S. National Academy of Science – National Research Council, Pub. 598, pp. 106–138.

Bronshteyn, V. K. and Chernov, A. A.: 1991, Freezing Potentials Arising on Solidification of Dilute Aqueous Solutions of Electrolytes, *J. Cryst. Growth* **112**, 129–145.

Engemann, S., Reichert, H., Dosch, H., Bilgram, J., Honkimaki, V. and Snigirev, A.: 2004, Interfacial Melting of Ice in Contact with SiO_2, *Phys. Rev. Lett.* **92**, 205701-1–4.

Groudieva, T., Kambourova, M., Yusef, H., Royter, M., Grote, R., Trinks, H. and Antranikian, G.: 2004, Diversity and Cold-Active Hydrolytic Enzymes of Culturable Bacteria Associated with Arctic Sea Ice, Spitsbergen, *Extremophiles,* in press

Inoue T. and Orgel, L.E.: 1982, Oligomerization of (Guanosine 5′-Phosphor)-2-Imidazolide on Poly(C): A Polymerase Model, *J. Mol. Biol.* **162**, 201–217.

Joyce, G.F.: 1987, Nonenzymatic Template-Directed Synthesis of Informational Macromolecules, *Cold Spring Harb. Symp. Quant. Biol.* **52**, 41–51.

Joyce, G.F., Inoue T. and Orgel, L.E.: 1984, Non-Enzymatic Template-Directed Synthesis on RNA Random Copolymers: Poly(C,U) Templates, *J. Mol. Biol.* **176**, 279–306.

Lohrmann, R. and Orgel, L. E.: 1976, Template-Directed Synthesis of High Molecular Weight Polynucleotide Analogs, *Nature* **261**, 342–344.

Lohrmann, R. and Orgel, L. E.: 1977, Reactions of Adenosine 5′-Phosphorimidazolide with Adenosine Analogs on a Polyuridylic Acid Template. The Uniqueness of the 2′-3′-Unsubstituted β-Ribosyl System, *J. Mol. Biol.* **113**, 193–198.

Macleod, G., McKeown, C., Hall, A. J. and Russell, M. J.: 1994, Hydrothermal and pH Conditions of Possible Relevance to the Origin of Life, *Origins Life Evol. Biosphere* **24**, 19–41.

Monnard, P., Apel, C. L., Kanavarioti, A. and Deamer, D. W.: 2002, Influence of Ionic-Inorganic Solutes on Self-Assembly and Polymerization Processes Related to Early Forms of Life: Implications for a Pre-Biotic Aqueous Medium, *Astrobiology* **2**, 139–152.

Monnard, P., Kanavarioti, A. and Deamer, D. W.: 2003, Eutectic Phase Polymerization of Activated Ribonucleotide Mixtures Yields Quasi-Equimolar Incorporation of Purine and Pyrimidine Nucleobases, *J. Am. Chem. Soc.* **125**, 13734–13740.

Moulton, V., Gardner, P. P., Pointon, R. F., Creamer, L. K., Jameson, G. B. and Penny, D.: 2000, RNA Folding Argues Against a Hot-Start Origin of Life, *J. Mol. Evol.* **51**, 416–421.

Munoz-Caro, G. G., Meierhenrich, U. J., Schutte, W. A., Barbier, B., Arcones-Segovia, A., Rosenbauer, H, Thiemann, W. H., Brack, A. and Greenberg, J. M.: 2002, Amino Acids from Ultraviolet Irradiation of Interstellar Ice Analogues, *Nature* **416**, 403–406.

Orgel L. E.: 1987, Evolution of the Genetic Apparatus: A Review, *Cold Spring Harbor Symp. Quant. Biol.* **52**, 9–16.

Sakshaug, E., Bjørge, A., Gulliksen, B., Løng, H. and Mehlum, F.: 1994, *Oekosystem Barenthavet*, Norges Forskningsrad Universitetsforlaget, Oslo, Norway.

Schwartz, A. W., Visscher, J., van der Woerd, R. and Bakker, C. G.: 1987, In Search of RNA Ancestors, *Cold Spring Harbor Symp. Quant. Biol.* **52**, 37–39.

Semiletov, I., Makshtas, A. and Akasofu, S.: 2004, Atmospheric CO_2 Balance: The Role of Arctic Sea Ice, *Geophys. Res. Lett.* **31**, 1–4.

Steponkus, P. L., Stout, D. G., Wolfe, J. and Lovelace, R. V. E.: 1984, Freeze-Induced Electrical Transient and Cryoinjury, *Cryo-Letters* **5**, 343–348.

Stribling, R. and Miller, S. L.: 1991, Template-Directed Synthesis of Oligonucleotides Under Eutectic Conditions, *J. Mol. Evol.* **32**, 289–295.

Trinks, H.: 2001a, *Leben im Eis*, Frederking and Thaler Verlag, Munich, Germany.

Trinks, H.: 2001b, *Auf den Spuren des Lebens (Origin of Life in Sea Ice)*, Shaker Verlag, Aachen, Germany.

Trinks, H., Schröder, W. and Biebricher, C. K.: 2003, *Eis und die Entstehung des Lebens*, Shaker Verlag, Aachen, Germany.

Vlassov, A. V., Johnston, B. H., Landweber, L. F. and Kazakov, S. A.: 2004, Ligation Activity of Fragmented Ribozymes in Frozen Solution: Implications for the RNA World, *Nucleic Acids Res.* **32**, 2966–2974.

Wettlaufer, J. S., Dash, J. G. and Untersteiner, N.: 1999, *Ice Physics and the Natural Environment*, Springer Verlag, Berlin, Germany.